The Egyptian Int. J. of Eng. Sci. and Technology
Vol. 16, No. 1 (Jan. 2013)

EIJEST

NUMERICAL STUDY OF PARTICLES GENERATION AND FLOW IN SiH_4/H_2 DISCHARGE*

Hala F. El Welily, Hany A. Abdel-Mohsen, Fatma El Tokhi**

Department of Physics and Mathematics, Faculty of Engineering, Zagazig University, Egypt.

ABSTRACT:

This paper contains a self consistent numerical study of fluid model in one dimension for the SiH_4/H_2 plasma discharge. Fluid model equations are solved for all species and particles specified in the model. Energy equation is solved only for electron species. The solution scheme is based on the explicit finite difference technique using Scharfetter-Gummel method for discretization. A coupling with a chemical model that investigate the nucleation and growth of all species contained in the discharge was performed. Different ion-ion, ion-molecule and molecule-molecule reactions leading to particle growth are taken into account. The results are focused on the average distribution of all species considered in the model and its flow inside the plasma bulk and at boundaries. The obtained results are of great agreement with other referred theoretical and experimental publications.

KEY WORDS*: Silane/Hydrogen Discharge, Fluid Model, Chemical Modeling.*

ETUDE NUMERIQUE DES GÉNÉRATION DE PARTICULES ET FLUX DE DÉCHARGE SIH4/H2

RÉSUMÉ:

Le présent document contient une étude de soi cohérente numérique de modèle fluide dans une dimension pour la décharge de plasma SiH4/H2. Équations du modèle sont résolues fluides pour toutes les espèces et les particules spécifiées dans le modèle. Équation de l'énergie est résolu que pour les espèces d'électrons. Le schéma de solution est basée sur la technique des différences finies explicite à l'aide Scharfetter-Gummel méthode de discrétisation. Un couplage avec un modèle chimique qui enquête sur la nucléation et la croissance de toutes les espèces contenues dans la décharge a été effectuée. Différentes réactions ion-ion, ion-molécule et molécule-molécule conduisant à la croissance des particules sont prises en compte. Les résultats portent sur la répartition moyenne de toutes les espèces prises en compte dans le modèle et son écoulement à l'intérieur de la masse à plasma et au niveau des frontières. Les résultats obtenus sont d'une grande concordance avec d'autres publications visées théoriques et expérimentales.

MOTS CLÉS: Décharge de silane / hydrogène, Modèle fluide, modélisation chimique.

* Received: 3/7/2012, Accepted: 11/10 /2012, Ref. No. 120, (Original Paper)

** Contact author (+2 0 1288234916)

1. INTRODUCTION

Plasma are quasi-neutral particle systems in the form of gaseous or fluid-like mixtures of free electrons, ions and neutral particles (atoms or molecules) (Rutscher[1] (2008)). It is almost found everywhere throughout the universe (Shafiq[2] (2006)). "*99% of the matter in the universe in the form of plasma*" (Shukla et al[3] (2002)). Much of the solid parts that appear in the universe are in the form of dust therefore (Shafiq[2] (2006)), plasma and dust coexist in the universe. "Pure" plasmas are complex systems of electrons, ions and neutral molecules interact with each other via collisions, chemical reactions and with the surroundings via the electromagnetic fields. In this sense, dust particles just introduce another degree of complexity in the dynamics of plasmas that's why it can expressed as "complex plasma" or "dusty plasma". It may be defined as the macroscopic charged micron-nano sized solid particles that appear in the normal ionized gas of plasma. These extra components may change the physical properties of the plasma and increase the complexity of the system. In spite of the harmful aspects of dust presence in plasma, the appearance of such fine produced and/or modified particles in plasma can be beneficial and have valuable properties for some specific applications such as the usage at the manufacturing of advanced nano-materials and electronic devices. These particles are no longer considered as impurities or unwanted pollutants.

The process of dust formation in silane plasma environment in the laboratory take place in three main steps, they are as in silane plasma (Perrin et al[4] (1996))

1) Initial nucleation which include the formation of short time clusters (2nm) with high concentration
2) Coagulation of small particles in which growth of the particles is up to 50-60 nm diameters
3) The growth of bigger particles of constant concentration due to the surface deposition of radicals in which we noticed a marked decrease in the electron concentration during the coagulation phase.

Our model investigates the physico-chemical reactions between different species which interacts with each other and with wall surface through surface deposition. It produces the average density distribution in the plasma bulk and at boundaries via solving fluid model equations.
First we produce the detailed chemistry modeling and then produce the fluid model equations.

2. PARTICLES STUDIED IN THE MODEL

Particles included in the model are listed in table (1).and sorted as ions, molecules and radicals. Positive ions, SiH_3^+, $Si_2H_4^+$, and H_2^+ formed from ionization of SiH_4, Si_2H_6, and H_2 are taken respectively. vibrationally excited silane molecules, formed by electron impact collision on ground state silane, are also considered. The first vibrational levels of silane SiH_4 $^{(2-4)}$, the bending modes at 0.113 eV, and SiH_4 $^{(1-3)}$, the stretching modes at 0.271 eV, are therefore incorporated as separate species.

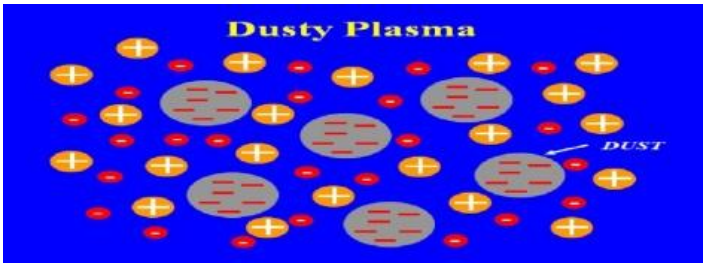

Fig. (1). Dusty plasma as amassive negative charged particles swimming in plasma of free electrons and positive ions.

Table (1), overview of different species included in the model

ions	Molecules	radicals
e^-,SiH_3^+, Si_2H4^+, H_2^+, [SiH_3^-, $Si_2H_5^-$, $Si_3H_7^-$$Si_4H_9^-$, $Si_5H_{11}^-$, $Si_6H_{13}^-$, $Si_7H_{15}^-$, $Si_8H_{17}^-$, $Si_9H_{19}^-$, $Si_{10}H_{21}^-$, $Si_{11}H_{23}^-$, $Si_{12}H_{25}^-$, **($Si_nH_{2n+1}^-$)],** [SiH_2^-, $Si_2H_4^-$, $Si_3H_6^-$, $Si_4H_8^-$, $Si_5H_{10}^-$ $Si_6H_{12}^-$, $Si_7H_{14}^-$, $Si_8H_{16}^-$,$Si_9H_{18}^-$, $Si_{10}H_{20}^-$, $Si_{11}H_{22}^-$, $Si_{12}H_{24}^-$,**($Si_nH_{2n}^-$)]**	**Excited species [** $SiH_4^{(1-3)}$, $SiH_4^{(2-4)}$, $H_2^{(v=1)}$, $H_2^{(v=2)}$, $H_2^{(v=3)}$**]** H_2 [SiH_4, Si_2H_6, Si_3H_8, Si_4H_{10}, Si_5H_{12},Si_6H_{14}, Si_7H_{16}, Si_8H_{18}, Si_9H_{20}, $Si_{10}H_{22}$, $Si_{11}H_{24}$, $S_{12}H_{26}$, **(Si_nH_{2n+2})]**	H [SiH_3,Si_2H_5, Si_3H_7, Si_4H_9, Si_5H_{11},Si_6H_{13}, Si_7H_{15}, Si_8H_{17}, Si_9H_{19} , $Si_{10}H_{21}$, $Si_{11}H_{23}$, $Si_{12}H_{25}$ **(Si_nH_{2n+1})]**, [SiH_2,Si_2H_4, Si_3H_6, Si_4H_8, Si_5H_{10},Si_6H_{12}, Si_7H_{14}, Si_8H_{16}, Si_9H_{18} , $Si_{10}H_{20}$, $Si_{11}H_{22}$, $Si_{12}H_{24}$ **(Si_nH_{2n})]**

3. ELECTRON COLLISIONS REACTIONS:

Initial reactions of electron impact with neutral background gases are responsible of the creation of different initial species (radicals, ions and molecules). These types of reactions require the threshold energy with the corresponding impact cross section (Hammond et al[5] (2002), Kurachi et al[6] (1989), Kortshagen et al[8] (1999) and De Bleecker et al[10] (2004)). Using these data for the calculation of the corresponding reaction rates and using the SIGLO data of Boeuf et al[9] (1996) an overview of the different electron impact reactions included in the model are listed in table (2) (De Bleecker et al[10,11] (2004).
The data obtained for cross sections of electron impact reactions are collected, fitted from experiments of Perrin et al[4], Mori et al and Wan etal, Tanaka et al, Chatham et al. Haaland et al[7] and Srivastava et al and then presented in details in Fig. (2,3)

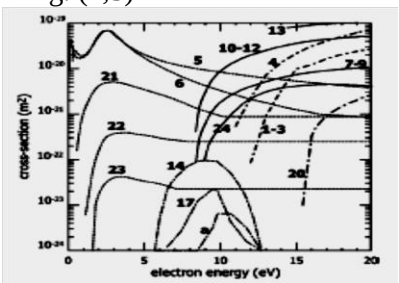

Fig. (2) Cross sections of electron collisions with SiH_4, H_2 and Si_2H_6 considerd in the model

The number of the reactions in table (2) is the same as those in the curve in Fig. (1). The cross section for the formation of SiH^- by dissociative attachment of SiH_4 (represented by curve *a*) is very low that this species is not taken into account in our model. Curves 14 and 17 represent the dissociative attachment of SiH_4 to produce SiH_3^- and SiH_2^-. And the dissociative attachment of vibrationally excited SiH_4 molecules is described by the same curves 14 and 17, are multiplied by a factor 10 to represent reactions 15,16,18,19 respectively in the electron impact table(2) (De Bleecker et al[10,11] (2004).

4. CHEMICAL REACTIONS:

The most important ion-molecule, molecule-molecule and ion-ion reactions are produced in Table (3) where the chemical reactions which are included in the model are given with their reaction rates. Some of the rates are a function of gas temperature or gas pressure as mentioned in the table and the estimated values represent the rates at 400K gas temperature and 40Pa gas pressures. As for reactions of anion-cation neutralization reactions included in the model as shown in table (3), Hickman et al derived a semi empirical formula for the calculation of the reaction rate constant as

$$N \approx (5.34 \times 10^{-13}) A_e^{-4} m_r^{-0.5} \left(\frac{T_{gas}}{300}\right)^{-0.5} \quad (1)$$

With A_e is the electron affinity (in eV) of the parent neutral species of the anion, m_r the reduced mass (in amu), and T_{gas} the gas temperature in kelvin. The solution of this equation induce that the reaction rates of this type of reactions slightly decrease from $1*10^{-13}$

for SiH_m^- up to $5*10^{-14}$ for $Si_{12}H_m$ (m=2n+1 or m=2n), therefore as an approximation the reaction rates are taken nearly $\approx 10^{-14}$ for this type of reactions

Table (2) An overview of different electron collision reactions

#	Reactions	Threshold energy(eV)	Reaction type
R1	$SiH_4 + e^- \rightarrow SiH_3^+ + H + 2e^-$	11.9	Diss-ionization
R2	$SiH_4^{(2-4)} + e^- \rightarrow SiH_3^+ + H + 2e^-$	11.8	Diss-ionization
R3	$SiH_4^{(1-3)} + e^- \rightarrow SiH_3^+ + H + 2e^-$	11.7	Diss-ionization
R4	$Si_2H_6 + e^- \rightarrow Si_2H_4^+ + 2H + 2e^-$	10.2	Diss-ionization
R5	$SiH_4 + e^- \rightarrow SiH_4^{(2-4)} + e^-$	0.11	Vib-excitation
R6	$SiH_4 + e^- \rightarrow SiH_4^{(1-3)} + e^-$	0.27	Vib-excitation
R7	$SiH_4 + e^- \rightarrow SiH_3 + H + e^-$	8.3	Dissociation
R8	$SiH_4^{(2-4)} + e^- \rightarrow SiH_3 + H + e^-$	8.2	Dissociation
R9	$SiH_4^{(1-3)} + e^- \rightarrow SiH_3 + H + e^-$	8.1	Dissociation
R10	$SiH_4 + e^- \rightarrow SiH_2 + 2H + e^-$	8.3	Dissociation
R11	$SiH_4^{(2-4)} + e^- \rightarrow SiH_2 + 2H + e^-$	8.2	Dissociation
R12	$SiH_4^{(1-3)} + e^- \rightarrow SiH_2 + 2H + e^-$	8.1	Dissociation
R13	$Si_2H_6 + e^- \rightarrow SiH_3 + SiH_2 + H + e^-$	7.0	Dissociation
R14	$SiH_4 + e^- \rightarrow SiH_3^- + H$	5.7	Diss-attachement
R15	$SiH_4^{(2-4)} + e^- \rightarrow SiH_3^- + H$	5.6	Diss-attachement
R16	$SiH_4^{(1-3)} + e^- \rightarrow SiH_3^- + H$	5.5	Diss-attachement
R17	$SiH_4 + e^- \rightarrow SiH_2^- + 2H$	5.7	Diss-attachement
R18	$SiH_4^{(2-4)} + e^- \rightarrow SiH_2^- + 2H$	5.6	Diss-attachement
R19	$SiH_4^{(1-3)} + e^- \rightarrow SiH_2^- + 2H$	5.5	Diss-attachement
R20	$H_2 + e^- \rightarrow H_2^+ + 2e^-$	15.4	Ionization
R21	$H_2 + e^- \rightarrow H_2^{(v=1)} + 2e^-$	0.54	Vib-excitation
R22	$H_2 + e^- \rightarrow H_2^{(v=2)} + 2e^-$	1.08	Vib-excitation
R23	$H_2 + e^- \rightarrow H_2^{(v=3)} + 2e^-$	1.62	Vib-excitation
R24	$H_2 + e^- \rightarrow H + H + 2e^-$	8.9	Dissociation

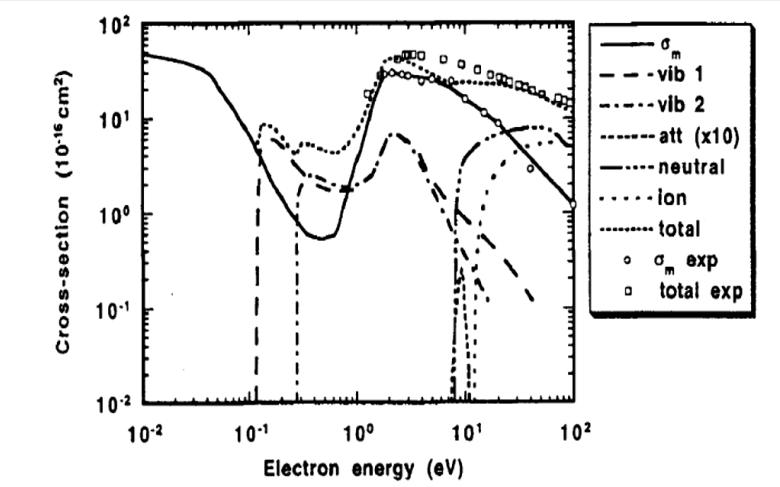

Fig. (3) Set of cross sections of electron impact on SiH_4 : The experimental data of **Tanaka** et al. for the elastic (momentum-transfer) cross-section and of Mori et al. for the total cross-section are shown for comparison

Table (3): the chemical reactions included in the SiH_4/H_2 model

Reactions	Rate constant (m^3/s)	Comment
Hydrogen abstraction		
$SiH_4+H \rightarrow SiH_3 + H_2$	1.2×10^{-18}	$2.8\times10^{-17}[\exp(-1250/T_{gas})]$
$Si_2H_6 + H \rightarrow Si_2H_5 + H_2$	7.0×10^{-18}	$1.6\times10^{-16}[\exp(-1250/T_{gas})]$
$Si_2H_6 + H \rightarrow SiH_3 + SiH_4$	3.5×10^{-18}	$0.8\times10^{-16}[\exp(-1250/T_{gas})]$
$[Si_nH_{2n+2} + H \rightarrow Si_nH_{2n+1} + H_2]$	1.1×10^{-17}	$2.4\times10^{-16}[\exp(-1250/T_{gas})]$ n=3,……,12
SiH_2 Insertion		
$SiH_2 + H_2 \rightarrow SiH_4$	2.7×10^{-20}	$3.0\times10^{-18}[1-(1+2.3\times10^{-4}p_0)^{-1}]$
$SiH_2 + SiH_4 \rightarrow Si_2H_6$	2.3×10^{-17}	$2.0\times10^{-16}[1-(1+0.0032p_0)^{-1}]$
$[SiH_2 + Si_nH_{2n+2} \rightarrow Si_{n+1}H_{2n+4}]$	4.9×10^{-17}	$4.2\times10^{-18}[1-(1+0.0033p_0)^{-1}]$ n=2,…….11
Neutral-Neutral reactions		
$Si_2H_5 + Si_2H_5 \rightarrow Si_4H_{10}$	1.5×10^{-16}	Estimated
$SiH_3 + SiH_3 \rightarrow SiH_2 + SiH_4$	1.5×10^{-16}	
Silyl anions ($Si_nH_{2n+1}^-$) reactions		
$[Si_nH_{2n+1}^- + SiH_4 \rightarrow Si_{n+1}H_{2n+3}^- + H_2]$	1.0×10^{-18}	Experimental
$[Si_nH_{2n+1}^- + SiH_4^{(2-4)} \rightarrow Si_{n+1}H_{2n+3}^- + H_2]$	1.0×10^{-18}	$10^{-18}\exp[(0.113eV)/RT]$
$[Si_nH_{2n+1}^- + SiH_4^{(1-3)} \rightarrow Si_{n+1}H_{2n+3}^- + H_2]$	2.6×10^{-17}	$10^{-18}\exp[(0.271eV)/RT]$ n=1,……11
Silylene anions ($Si_nH_{2n}^-$)		
$[Si_nH_{2n}^- + SiH_4 \rightarrow Si_{n+1}H_{2n+2}^- + H_2]$	1.0×10^{-15}	Experimental
$[Si_nH_{2n}^- + SiH_4^{(2-4)} \rightarrow Si_{n+1}H_{2n+2}^- + H_2]$	1.0×10^{-18}	$10^{-18}\exp[(0.113eV)/RT]$
$[Si_nH_{2n}^- + SiH_4^{(1-3)} \rightarrow Si_{n+1}H_{2n+2}^- + H_2]$	2.6×10^{-17}	$10^{-18}\exp[(0.271eV)/RT]$ n=1,……11
Neutralization of silyl & silylene		
$[Si_nH_{2n+1}^- + SiH_3^+ \rightarrow Si_nH_{2n+1} + SiH_3]$	$\approx10^{-14}$	Calculated
$[Si_nH_{2n+1}^- + Si_2H_4^+ \rightarrow Si_nH_{2n+1} + 2SiH_2]$	$\approx10^{-14}$	Calculated
$[Si_nH_{2n}^- + SiH_3^+ \rightarrow Si_nH_{2n} + SiH_3]$	$\approx10^{-14}$	Calculated
$[Si_nH_{2n}^- + Si_2H_4^+ \rightarrow Si_nH_{2n} + 2SiH_2]$	$\approx10^{-14}$	Calculated n=1,……12
Deexcitation of vib-excited SiH_4		
$SiH_4+SiH_4^{(2-4)} \rightarrow 2\ SiH_4$	1.0×10^{-18}	Interpolation
$SiH_4+SiH_4^{(1-3)} \rightarrow 2\ SiH_4$	1.2×10^{-18}	Interpolation
$H_2+SiH_4^{(2-4)} \rightarrow SiH_4 + H_2$	3.7×10^{-18}	Interpolation
$H_2+SiH_4^{(1-3)} \rightarrow SiH_4 + H_2$	4.1×10^{-18}	Interpolation

5. SPECIES DIFFUSION AND MONILITY (TRANSPORT) COEFFICIENTS

For the neutral particles the mobility is set equal to zero. The diffusion constant D_j of neutral particle *j* in the background gases *i* (SiH_4, H_2 and Si_2H_6) is calculated by first determining the separate binary diffusion coefficient D_{ij} using the following expression.

$$D_{ij} = \frac{3k_B T_g \sqrt{2\pi k_B T_g / m_{ij}}}{16\pi P_i \sigma_{ij}^2\, \Omega_D(\Psi)} \qquad (2)$$

Where p_i is the partial pressure of background species *i*, m_{ij} is the reduced mass , σ_{ij} is the binary collision and the paramerte $\Omega_D(\Psi)$ is The Lennard-Jones parameters are taken from G. J. Nienhuis et al[12] (1997) and J. Perrin et al[4] (1996). The diffusion coefficient *Dj* of particle *j* in the background gas mixture *i* is then approximated using Blancs law.

$$\frac{p_{tot}}{D_j} = \sum_i \frac{p_i}{D_{ij}} \qquad (3)$$

The ion mobility coefficients in the background gas mixture are similarly calculated as the diffusion coefficients of the neutrals. The ion mobility of ion *j* in background neutral *i*(SiH_4,

H_2 and Si_2H_6) is calculated using the low E-field Langevin mobility expression,

$$\mu_{ij} = 0.514 \frac{T_g}{p_{tot}} \left(\alpha_i m_{ij}\right)^{-0.5} \quad (4)$$

Where α_i is the polarizability of background neutral gas *i*. Similarly the ion mobility in the mixture is again obtained using Blanc's law.

$$\frac{p_{tot}}{\mu_j} = \sum_i \frac{p_i}{\mu_{ij}} \quad (5)$$

The ion diffusion coefficient is then calculated using the Einstein relation,

$$D_i = \frac{K_B T_{ion}}{e} \mu_i \quad (6)$$

Where T_{ion} is the ion temperature which is assumed to be equal to the gas temperature T_{gas}. The expression of the ion mobility shows that m_j, and hence also D_j, decrease with cluster size as well.

6. FLUID MODEL EQUATIONS:

It is necessary to simulate fluid model self-consistently to ensure coupling between particles growth and changes in plasma parameters (De Bleecker et al[13] (2006)). The fluid model describes the plasma discharge between two parallel electrodes in one dimension perpendicular to the electrodes. The fluid equations of plasma are derived from the Boltzmann equation for each species (electron, ion and neutrals) by specifying the velocity distribution function and by taking the velocity moment of Boltzmann equation leading to the final form called drift-diffusion equation as Tapia et al[14] (2006), Salabas[15] (2003):

$$\frac{\partial n_p}{\partial t} + \nabla . \Gamma_p = S_p \quad (7)$$

$$\Gamma_p = -D_p \nabla n_p - \mu_p n_p E \quad (8)$$

where the subscript p indicates every particle in the discharge, n_p is the species number density, Γ_p is the particle flux consists of two terms diffusion term (caused by density gradients) and drift term (caused by electric field), D_p , μ_p are species diffusion and mobility parameters respectively, E is the electric field, finally S_p is the species source term and can be written as

$$S = S_{react} + S_{flow} + S_{pumping} \quad (9)$$

S_{react} Represents the source term of the creation or destruction of corresponding particle through electron impact collisions with neutrals and/or by chemical reactions.

$$S_{react} = k_{react} n_{p1} n_{p2} \quad (10)$$

S_{flow} , $S_{pumping}$ are the inlet of the feed gases and the pumping in the deposition reactor, respectively.

Electric field is obtained by solving the Poisson's equation

$$\nabla^2 V = -\frac{e}{\varepsilon_0} \left(\sum_{i=ion} q_i n_i - n_e\right) \quad (11)$$

$$E = -\nabla . V \quad (12)$$

Where, q_i indicates the sign of the corresponding ion.

Energy balance equation is solved for electron not including energy balances for ions or neutrals. It is assumed that the ions have nearly the same energy as the neutral atoms, because of the efficient energy transfer between ions and neutrals due to their nearly equal mass. Further, the energy gain of the ions from the electric field is low because of the high inertia of the ions.

$$\frac{\partial w_e}{\partial t} + \nabla . J_w = -e\Gamma_e . E - S_w \quad (13)$$

$$J_w = -\frac{5}{3} D_e \nabla w_e - \frac{5}{3} \mu_e w_e E \quad (14)$$

$$w_e = n_e \varepsilon \quad (15)$$

$\boldsymbol{J_w}$ is the electron energy flux, $\boldsymbol{w_e}$ Is the total electron energy density , $\boldsymbol{(\nabla . J_w)}$ is convective transport term of energy and $\boldsymbol{(e\Gamma_e . E)}$ is ohm heating source term. The term $\boldsymbol{S_w}$ in the electron energy balance equation is the loss of electron energy due to electron impact collisions.

Boundary Conditions And Surface Reactions: These set of fluid model equations are solved with certain boundary conditions for the potential and density profiles. The potential is set for boundaries at each electrode where at the grounded electrode (x=0) is equal to zero, and at the powered electrode the potential is set at

$$V(x = l, t) = V_{rf} \sin(2\pi\omega t) \quad (16)$$

$\boldsymbol{\omega}$ is the frequency of the oscillating potential, $\boldsymbol{V_{rf}}$ is the amplitude of the potential.

The density profile can be expressed by the mass transfer to the wall (plasma-wall interaction model). For negative ions and electron the density gradient are set to be zero, they are

trapped in the plasma and then the ion flux at the electrodes has only a drift component. Only positive ions that can cross the plasma sheath and reach the wall. As for neutral species a model of plasma-wall interaction via surface deposition is used which is modeled using the equation of flux at any solid surface (electrode, reactor wall) Perrin et al[4] (1996), Nienhuis et al[12] (1997), De Bleecker et al[16] (2003)and Maurice et al[17] (2002). Only the radicals react with the surface while non-radical neutrals (H_2, SiH_4, Si_2H_6 and Si_nH_{2m+2}) are reflected into the discharge and do not react at the surface.

$$D_i \left|\frac{\partial n_i}{\partial x}\right|_{surface} = \pm n_i \sqrt{\frac{k_B T}{2\pi m_i}} \left(\frac{\beta_i}{1-\beta_i}\right) \quad (17)$$

$$\frac{V_{th}}{4} = \sqrt{\frac{k_B T}{2\pi m_i}} \quad (18)$$

As the parameter $\boldsymbol{\beta_i}$ is the loss probability, i.e. the probability of the particle to be lost at the surface which is the sum of two main parameters, sticking probability $\boldsymbol{s}$ (probability of the particle to stick on the surface and contribute to the thin film growth by Si incorporation) and Recombination probability $\boldsymbol{\gamma}$ (the probability that the particle react with another absorbed species on the surface to form a stable volatile product). For SiH_3, the loss probability β was measured and set at 0.26 with sticking coefficient of 0.09. The surface reaction coefficients of Si_nH_{2n+1}, where $n>1$, is scarce. Because the structure of these radicals is similar to that of SiH_3, the same surface reaction coefficients are used. It is assumed that if Si_nH_{2n+1} radical recombine at the surface with a hydrogen atom, a Si_nH_{2n+2} neutral is formed which is reflected into the discharge. For SiH_2, we assume large β and $s = \beta$ at 0.8 since there is no barrier for insertion of these species into Si-H surface bond on the growing film and radicals of Si_nH_{2n} are assumed to have the same surface reaction coefficients as SiH_2. For H atom $\beta = \gamma = 0.7$

7. RESULTS AND DISCUSSION

The calculated average density profiles obtained from the one dimensional fluid model of each species in the modeling with a brief discussion are now presented in the following figures in (cm^{-3}) and for simplicity the figures are sorted into groups as positive ions profile, negative ions profiles, neutral molecules, radicals profile and excited states profiles are also presented. The results is a numerical simulation of experimental set up of parallel plates, capacitively coupled radio frequency (50 MHz) Rf glow discharge of 3 cm electrode spacing, 20 sccm for silane flow and 20 sccm for Hydrogen flow. Modeling operated and all calculations are made for 40 Pa pressure, 400 K gas temperature and 5W power.

And the chemical simulation is processed at rate coefficients of electron impact reactions calculated from the cross sections of impact as a function of electron energy using SIGLO series of cross section and gas parameters. Other rates of chemical reactions are presented as function of either gas temperature or pressure of the indicated values or calculated with certain mentioned procedure. a rate constant of $10^{-18} m^3 sec^{-1}$is used for the ground state SiH_4-anion reactions. And used in the calculations of the rates of vibrationally excited molecules-anions reactions.

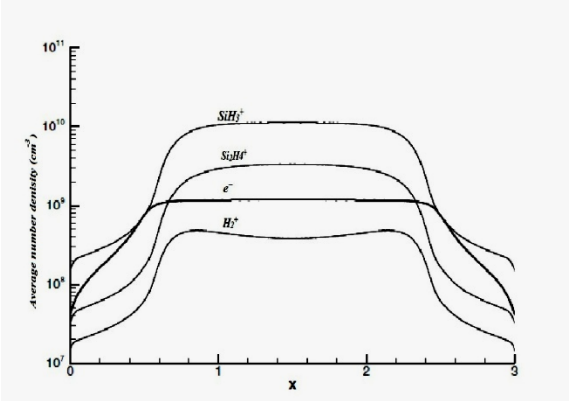

Fig. (4) Electron and positive ions density profile.

As appears from the calculated density profile in Fig.(4) that, inside the plasma bulk, the most positive ion appears to be SiH_3^+ with density in the order of 10^{10} cm^{-3} followed by $Si_2H_4^+$ with lower density profile of 4×10^9 cm^{-3} as SiH_3^+ is produced in the system from dissociative ionization of ground state SiH_4 and of the two excited states SiH_4^{**} at threshold energy of 11.9eV while $Si_2H_4^+$ is a product of dissociative ionization of disilane Si_2H_6 at

threshold energy of 10.2 eV. And both is consumed at the same reactions of ion-anion neutralization at the same values of reaction rates. But for H_2^+ density is much lower of a value of 5×10^8 cm^{-3} as they are only produced in the system from electron impact with H_2 at high threshold energy of 15.4 eV and it is assumed according to the involved reactions that it doesn't undergo any ion-ion neutralization reactions. The electron density profile is of the order of 10^9 cm^{-3} inside the discharge bulk.

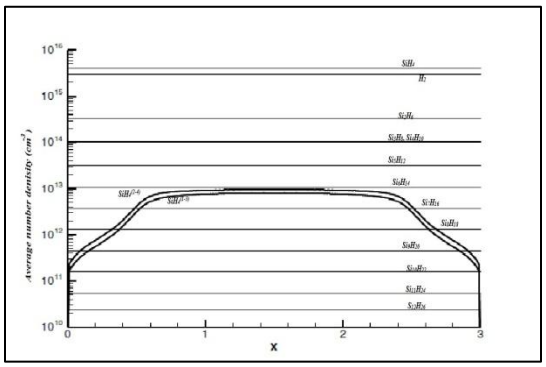

Fig. (5) Density profile of neutral background molecules, Si_nH_{2n+2} and excited molecules of SiH_4.

The number density profile of the background species is homogeneously distributed over the spacing between electrodes (plasma bulk & sheath) as obvious in Fig. (5). These molecules have no variance or change in the sheath region because according to the boundary conditions they have no surface reactions as explained before. The same profile calculated for the neutral molecules of Si_nH_{2n+2} for n > 2. The background gas SiH_4 is the highest density profile of 4×10^{15} cm^{-3}, Followed by H_2 gas with density profile of about 3×10^{15} cm^{-3}. This density is relatively high but reasonable according to many included reactions that cause Hydrogen creation like H-abstraction, silyle and silylene anion reactions with SiH_4 and with its excited states and finally deexcitation reactions, that's beside the hydrogen reflected into the discharge bulk from the sticking of radicals at the surface of the reactor. After then appears the density profile of Si_2H_6 with value of about 3×10^{15} cm^{-3}. The density profile of higher order silane Si_nH_{2n+2} for n > 2 after then is ordered with n=3,4,5…… 12. These particles productions come from the SiH_2 insertion reactions as shown in the table of chemical reactions while it is absorbed in the H-abstraction reactions. In contrary to SiH_4 very high density values the excited states $SiH_2^{(2\text{-}4)}$, $SiH_2^{(1\text{-}3)}$ density profile is very low of values 5×10^{12} and 4×10^{12} cm^{-3} inside the plasma bulk.

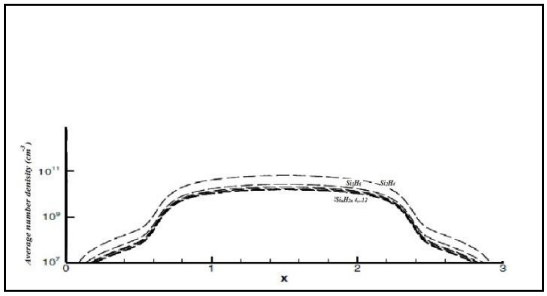

Fig. (6) Density profile of neutral radicals silylene Si_nH_{2n} in Silane discharge.

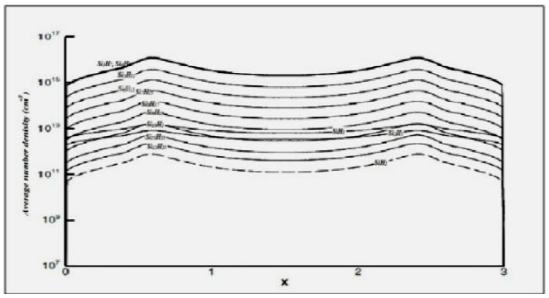

Fig. (7) Density profile of neutral radicals silyl (Si_nH_{2n+1}) in Silane discharge.

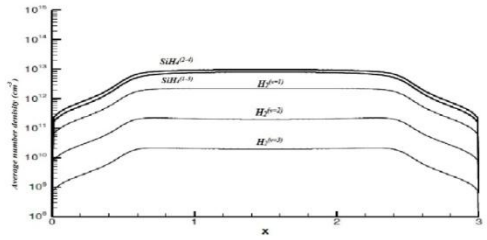

Fig. (8) Density profile of Hydrogen and Silane excited states

In Fig. (7), the Si_nH_{2n+1} silyl radicals density profile is produced. The most important radical is SiH_3. It is responsible of the initial growth procedure. For the silylene radicals as shown in the calculated density curve, in dashed lines, in Fig. (6) they are the lowest density profile and they all have the same density concentration.

This may be explained that they all products of the neutralization reactions of their anions

$$Si_nH_{2n}^- + SiH_3^+ \rightarrow Si_nH_{2n} + SiH_3$$

$$Si_nH_{2n}^- + Si_2H_4^+ \rightarrow Si_nH_{2n} + 2SiH_2$$

These reactions are approximated to have the same production rates. As radicals they have no other reactions in the model. They are incorporated in the model because of their anions have important reactions in the dust production.

In our model we considered the hydrogen excited states as separate species and calculate their density profile as in Fig. (8). As obvious they are of low density because they only products from vibrationally excitation reactions of different threshold energy of 0.54, 1.08 and 1.62 eV and different cross sections.

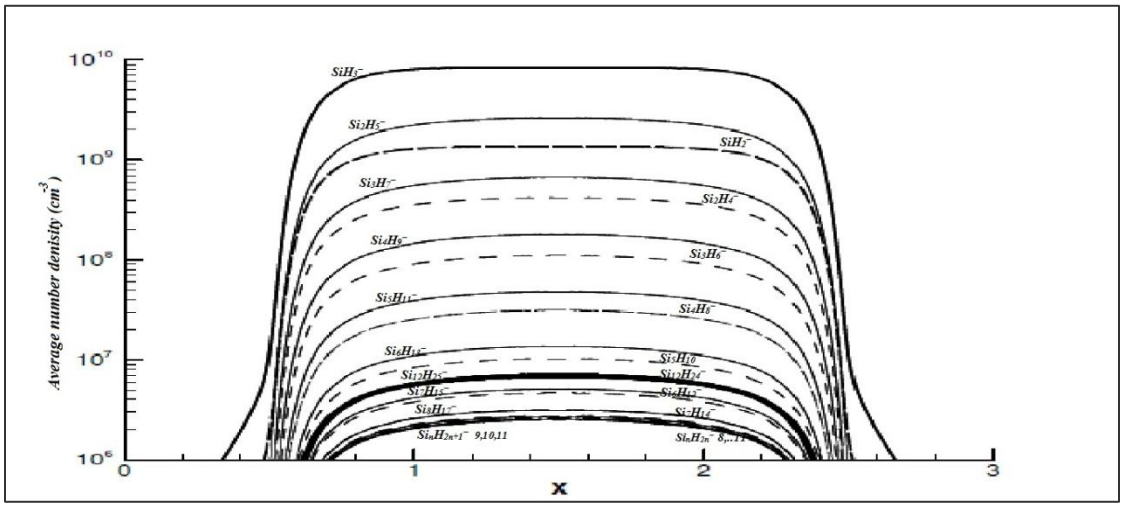

Fig. (9) Anion silyle ($Si_nH_{2n+1}^-$ in solid lines) and silylene ($Si_nH_{2n}^-$ in dashed lines) density profile.

The density profile of anion silyle ($Si_nH_{2n+1}^-$ in solid lines) and silylene ($Si_nH_{2n}^-$ in dashed lines) are produced in Fig. (9). It is obvious from the very high density concentration of the negative ion clusters of silyl and silylenes inside the discharge bulk that the silane discharge is a negative dust formation reactor. especially the high density of SiH_3^- and SiH_2^- about 6×10^9 and 9×10^8 respectively, i.e. two order of magnitude higher than electron density profile. Inside the sheath, according to the low electric field the negative ions boundary conditions are set that they cannot cross the sheath and reach the surface that's why there are no ions appears in the sheath region.

From The silyle anions and silylene anions reactions growth pathway produced in table (3) we can see that in each reaction ion radical, silyl & silylene, of (n) Silicon atoms is consumed and lost in the reaction to give birth of higher order (n+1) Silicon atoms which is also lost in the next reaction in the same growth pathway. These ions are consumed only in the mutual neutralization with SiH_3^+ and $Si_2H_4^+$. All that give reasonable gradual ordering of these species from n=1 up to n=11, but for n=12 it is little higher in density and this back to that reaction are cut at $Si_{12}H_m$ species as a product (construction) and undergoes no consuming reaction (destruction).

8. CONCLUSIONS

A self consistent one dimensional fluid model fluid model based on chemical reactions nucleation phase of dust formation is investigated to model the particles nucleation and formation in low-pressure Hydrogen-Silane plasma. The model was operated through two main parts; the first was modeling fluid equation (drift diffusion, flux, Poisson's and electron energy equation) of a low pressure parallel

plates capacitively coupled Rf SiH_4/H_2 discharge. The second part based on modeling the chemical formation and destruction of each species incorporated in the model. The model contained 71 species react through 169 reactions with a detailed discussion of causes below choice of each species. Besides the main electron impact reactions and main chemical reactions that affect initial particle formation and growth are also discussed with their electron impact cross sections and chemical reaction rates involved. Particle nucleation presented in the results through the time average number density distribution over the space between two electrodes (plasma bulk and sheath). A brief discussion on each curve of the results is presented which came in great accuracy with publications. It is obvious from results that electron density inside the discharge relatively low due to electron loss in attachment reactions. The molecule-molecule reactions found to be of lower affect on particles growth and the most important reactions are ion-molecule reactions. The anion SiH_3^- is the most important species that starts the particle formation through silyl anions $Si_nH_{2n+1}^-$ reactions with ground state silane and with its excited states which are the main reactions pathway of particle formation. Particles growth via silylene anion $Si_nH_{2n}^-$ reactions starting with SiH_2^- are also calculated but appear to be of lower density profile. While radicals Si_nH_{2n+1}, Si_nH_{2n} are the main species that are responsible of the thin film Si-H growth through producing Si deposition of surface reactions while negative ions trapped inside the discharge.

REFERENCES

[1]Alfred Rutscher, characteristics of low temperature plasma under nonthermal conditions, Wiley, ISBN: 978-3-527-40673-9.

[2]Muhammed Shafiq, PHD. Thesis, Test Charge Response of a Dusty Plasma with Grain Size Distribution and charging Dynamics, Stockholm (2006).

[3]P. K. Shukla, A. A. Mamoun, Fundamental Of Plasma Physics, Institute of Physics,(2002), ISBN:0 7503 0653 X

[4] J. Perrin, O. Leroy and M. C. Bordage, Cross Section, Rate Constants and Transport coefficients in Silane Plasma Chemistry, Contrib. Plasma Phys. 36 (1996) 1, 3-49.

[5] E. P. Hammond, K. Mahesh and P. Moin ,A Numerical Method to Simulate Radio-Frequency Plasma Discharges, Jour. Comp. Phys. 176, 402–429 (2002).

[6] M Kurachi and Y Nakamura, Electron collisions cross sections for the monosilane molecule, J. Phys. D: Appl. Phys. 22 107 (1989).

[7] Peter Haaland, Dissociative attachment in silane, J. Chem. Phys. 93, 4066 (1990).

[8] U. R. Kortshagen, U. V. Bhandarkar, M. T. Swihart and S. L. Girshick, Generation and growth of nanoparticles in low-pressure plasmas, Pure Appl. Chem., Vol. 71, No. 10, pp. 1871-1877(1999).

[9] J. P. Boeuf and L. C. Pitchford, the SIGLO Series, Gas parameters and cross sections data, (1996).

[10] Kathleen De Bleecker, Annemie Bogaerts, and Renaat Gijbels, Numerical investigation of particle formation mechanisms in silane discharges, Physical Review E 69, 056409 (2004).

[11] Kathleen De Bleecker, Annemie Bogaerts, Wim Goedheer, and Renaat Gijbels, Investigation of Growth Mechanisms of Clusters in a Silane Discharge With the Use of a Fluid Model

[12] G. J. Nienhuis, W. J. Goedheer, E. A. G. Hamers, W. G. J. H. M. van Sark and J. Bezemer,A self-consistent fluid model for radio-frequency discharges in SiH4–H2 compared to experiments, J. Appl. Phys. 82, 2060 (1997).

[13] Kathleen De Bleecker, Annemie Bogaerts and Wim Goedheer, Modeling of nanoparticle coagulation and transport dynamics in dusty silane discharges, New Journal of Physics 8 (2006) 178.

[14] Eduardo Rodrigo Gonzalez Tapia, Analysis, modeling and Numerical Simulation of Complex Plasmas Under Microgravity Conditions, Munchen (2006).

[15] Aurel Salabas, Fluid model for charged particle transport in capacitively coupled radio-frequency discharges, Master thesis, University technology of Lisboa, October 2003.

[16] K. De Bleecker., D Herreb, A. Bogaerts, R. Gijbels and P. Descamps, One-dimensional modelling of a capacitively coupled rf plasma in silane/helium, including small concentrations of O2 and N2, J. Phys. D: Appl. Phys. 36 (2003) 1826–1833.

[17] Maurice H. Francombe, Thin Films and Nanostructures, Advances in plasma grown hydrogenated films, Handbook, volume 30, (2002).